Arid3a is essential to execution of the first cell fate decision via direct embryonic and extraembryonic transcriptional regulation

Catherine Rhee,[1,2] Bum-Kyu Lee,[1,2] Samuel Beck,[1,2] Azeen Anjum,[1] Kendra R. Cook,[1] Melissa Popowski,[1,2] Haley O. Tucker,[1,2] and Jonghwan Kim[1,2,3]

[1]Department of Molecular Biosciences, [2]Institute for Cellular and Molecular Biology, [3]Center for Systems and Synthetic Biology, The University of Texas at Austin, Austin, Texas 78712, USA

Despite their origin from the inner cell mass, embryonic stem (ES) cells undergo differentiation to the trophectoderm (TE) lineage by repression of the ES cell master regulator Oct4 or activation of the TE master regulator Caudal-type homeobox 2 (Cdx2). In contrast to the in-depth studies of ES cell self-renewal and pluripotency, few TE-specific regulators have been identified, thereby limiting our understanding of mechanisms underlying the first cell fate decision. Here we show that up-regulation and nuclear entry of AT-rich interactive domain 3a (Arid3a) drives TE-like transcriptional programs in ES cells, maintains trophoblast stem (TS) cell self-renewal, and promotes further trophoblastic differentiation both upstream and independent of Cdx2. Accordingly, *Arid3a*$^{-/-}$ mouse post-implantation placental development is severely impaired, resulting in early embryonic death. We provide evidence that Arid3a directly activates TE-specific and trophoblast lineage-specific genes while directly repressing pluripotency genes via differential regulation of epigenetic acetylation or deacetylation. Our results identify Arid3a as a critical regulator of TE and placental development through execution of the commitment and differentiation phases of the first cell fate decision.

[*Keywords*: Arid3a; trophoblast stem cells; embryonic stem cells; trophectoderm; first cell fate decision; *trans*-differentiation]

Supplemental material is available for this article.

Received June 10, 2014; revised version accepted September 17, 2014.

Transformation of a totipotent zygote into a multilineage blastocyst encompasses a series of cellular, morphological, and molecular events required for implantation and development into an offspring (Zernicka-Goetz et al. 2009). Three distinct cellular lineages—the trophectoderm (TE), the epiblast, and the primitive endoderm—comprise the early developing embryo. Two sequential cell fate decisions during blastocyst formation are required to establish these lineages. The first cell fate decision, occurring at the 16- to 32-cell stage, leads to segregation of the TE and inner cell mass (ICM). The TE is required for implantation into the uterus and formation of the placenta, whereas the cells in the ICM are pluripotent and have the capacity to give rise to all tissues and organs in the body (Niwa 2007). The second cell fate decision controls division of the ICM into the epiblast and the primitive endoderm.

Since embryonic stem (ES) cells are derived from the ICM (Evans and Kaufman 1981), intensive studies have identified crucial ES cell "core" transcription factors (TFs) such as Oct4, Sox2, and Nanog that are central to the construction of a sophisticated transcriptional regulatory circuit termed the "core pluripotency network." TFs within the circuitry work in concert to allow ES cells to self-renew while maintaining pluripotency, primarily by activating pluripotency-associated genes and repressing lineage-specific TFs (Kim et al. 2008). In contrast, only a few TFs required for TE specification have been identified, and much less is understood as to how they orchestrate the segregation of the ICM and TE during the first cell fate decision (Zernicka-Goetz et al. 2009). The first cell fate can be divided into four phases: specification, commitment, maintenance, and differentiation (Nishioka et al. 2008; Pfeffer and Pearton 2012). The current consensus suggests that specification of the first cell fate, which occurs prior to implantation, is activated

Corresponding authors: jonghwankim@mail.utexas.edu; haleytucker@austin.utexas.edu

Article is online at http://www.genesdev.org/cgi/doi/10.1101/gad.247163.114. Freely available online through the *Genes & Development* Open Access option.

by the Hippo signaling pathway (Nishioka et al. 2009). Nuclear localization of Yap following Hippo repression by Notch in "outer" cells results in the activation of critical TE gene expression through interaction with Tead4 (Rayon et al. 2014). This leads to sustained and restricted expression of Caudal-type homeobox 2 (Cdx2) and initiation of the commitment stage of the first cell fate decision. Cdx2 is broadly expressed during preimplantation development (eight- to 16-cell stage) but becomes restricted to the outer cells of the TE during blastocyst formation (Dietrich and Hiiragi 2007). *Cdx2*$^{-/-}$ embryos develop to the blastocyst stage but fail to maintain their morphology and do not implant (Strumpf et al. 2005). Oct4 is essential for establishing embryonic pluripotency (Nichols et al. 1998; Strumpf et al. 2005) and, while broadly expressed at the same stages, becomes restricted to the ICM (Dietrich and Hiiragi 2007). Accordingly, *Oct4*$^{-/-}$ embryos fail to establish a functional ICM (Nichols et al. 1998).

Studies in both preimplantation embryos and ES cells have established an antagonistic relationship between Cdx2 and Oct4 during TE commitment. Knockout or knockdown of Cdx2 permits expression of Oct4 in the TE lineage (Strumpf et al. 2005; Wu et al. 2010), whereas overexpression (OE) of Cdx2 or knockdown of Oct4 in ES cells induces TE differentiation (Niwa et al. 2005). Similarly, OE of Cdx2 or the additional TE-restricted TF Gata3 or Tcfap2c promotes transition of ES cells into trophoblast stem (TS)-like cells, which are similar to an in vitro counterpart of TE derived from preimplantation embryos (Kuckenberg et al. 2010; Ralston et al. 2010). In contrast, OE of Oct4 in TS cells promotes an ES cell-like fate (Wu et al. 2011). Several factors preferentially expressed in the TE (e.g., Cdx2, Gata3, and Tcfap2c) are involved in self-renewal of TS cells (Chawengsaksophak et al. 1997; Auman et al. 2002; Ralston et al. 2010). Although the antagonistic regulatory mechanism between Cdx2 and Oct4 has been widely accepted from results obtained from mouse ES cells, whether they directly repress each other remains controversial (Niwa et al. 2005; Nishiyama et al. 2009).

Most TFs within the pluripotency network of ES cells are coordinately down-regulated upon exit from the self-renewal program, with only a few factors up-regulated. AT-rich interactive domain 3a (Arid3a)/Bright/Dril1 is one such pluripotency network factor whose modest expression in self-renewing ES cells is dramatically up-regulated upon differentiation (Wang et al. 2006). Arid3a, the founding member of the ARID family of TFs, has been characterized as a transactivator of both B lymphocyte development and cell cycle progression (Herrscher et al. 1995). Loss-of-function studies revealed that >98% of *Arid3a*$^{-/-}$ mice die prior to embryonic day 11.5 (E11.5) (Webb et al. 2011), suggesting a potential role in embryonic development. A recent follow-up study showed that singular loss of *Arid3a* is sufficient for reprogramming as well as enhancement of standard four-factor reprogramming of mouse embryonic fibroblasts (MEFs) to fully induced pluripotent stem cells (Takahashi and Yamanaka 2006; Popowski et al. 2014). That Arid3a is expressed highly in extraembryonic trophoblast lineages that give rise to the placenta (Wu et al. 2009) led us to examine its function in ES cells and TE lineage commitment and differentiation.

Here, we present evidence that Arid3a is a critical transcriptional regulator of ES to TS-like cell *trans*-differentiation and plays an important role in the commitment and differentiation of TE rather than its specification. Induction of Arid3a in ES cells or bona fide blastula-derived TS cells triggers the TE-specific gene expression program and differentiation toward subsequent trophoblastic lineages, whereas knockdown of Arid3a compromises differentiation of ES cells. When injected into four- to eight-cell stage embryos, Arid3a OE-generated TS-like cells adopt an outside cell fate, synonymous with commitment to the TE lineage. Intersection of global gene expression, genome-wide target mapping, and cellular localization studies revealed that, upon nuclear up-regulation, Arid3a acts both directly upstream of and parallel to *Cdx2* to activate key TE-specific genes while directly repressing regulators of ES cell pluripotency, including *Oct4* and *Nanog*. Arid3a and histone deacetylases 1/2 (HDAC1/2) associate at the protein level and selectively co-occupy regulatory regions of pluripotent genes, suggesting a mechanism by which differential Arid3a complexes contribute to execution of the first cell fate decision.

Results

Arid3a is dispensable for mouse ES cell self-renewal but critical for normal differentiation

In order to elucidate the function of Arid3a in self-renewal and differentiation, we first performed a shRNA-based knockdown of Arid3a in the mouse ES cell line J1. We obtained >75% knockdown efficiency at both the protein and mRNA levels (Fig. 1A; Supplemental Fig. S1A). Arid3a-deficient cells displayed normal ES cell morphology as well as alkaline phosphatase (AP) activity and proliferation rates comparable with control cells (Fig. 1B; Supplemental Fig. S1B). While knockdown of Arid3a resulted in modest up-regulation of mRNA levels of previously established ES cell core pluripotency factors, including Oct4, Sox2, and Nanog (Supplemental Fig. S1A), we observed no significant changes in the protein levels of these factors (Fig. 1A). These data indicate that Arid3a is dispensable for self-renewal of ES cells.

Unlike the majority of TFs comprising the ES cell pluripotency network, Arid3a is moderately expressed in undifferentiated ES cells but significantly induced upon differentiation (Supplemental Fig. S1C). To test the potential function of Arid3a during differentiation, we cultured Arid3a knockdown ES cells and normal ES cells in differentiation medium (leukemia inhibitory factor [LIF] withdrawal). While control ES cells showed differentiated morphology with reduced rates of growth, Arid3a-deficient ES cells maintained undifferentiated cell morphology for about five additional days, with proliferation rates similar to those of control ES cells under

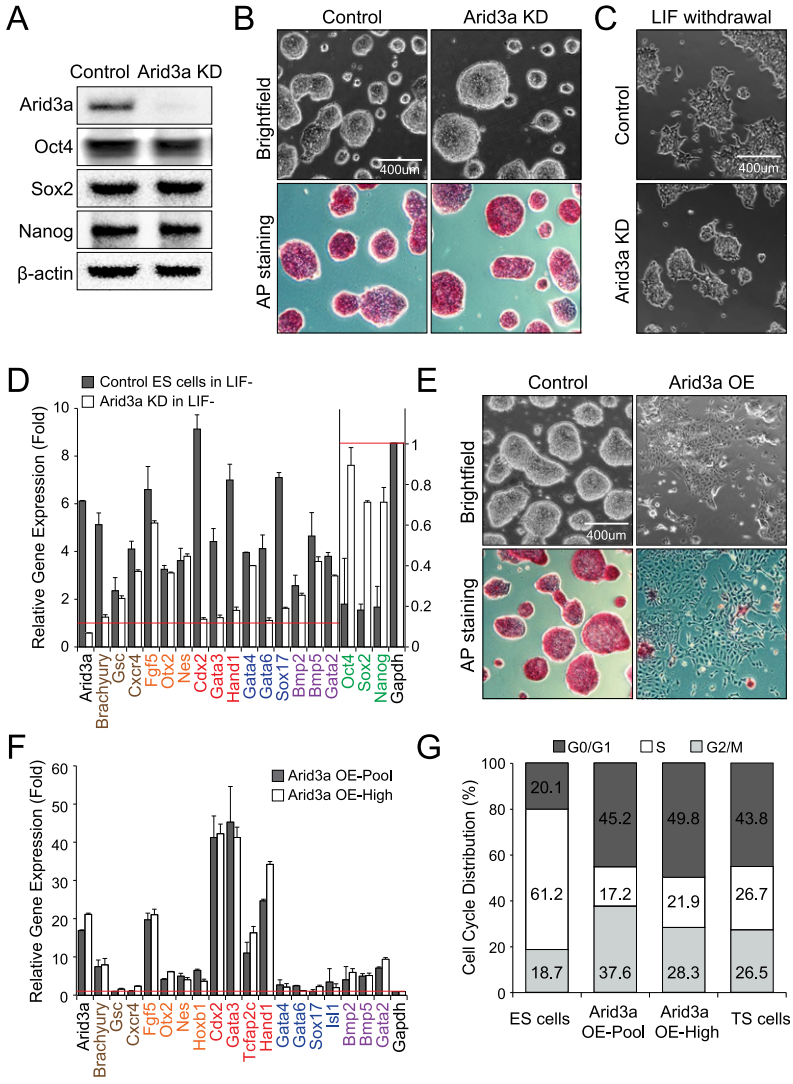

Figure 1. Arid3a is critical in ES cell differentiation. (*A*) Protein levels of the pluripotency-associated TFs Oct4, Sox2, and Nanog following Arid3a knockdown (KD) as measured by Western blotting. β-Actin was the loading control. (*B*) ES cell morphology upon knockdown of Arid3a. Arid3a knockdown cells were plated at clonal density, cultured for 5 d, and stained for AP. (*C*) ES cell morphologies of control ES cells and Arid3a knockdown cells upon LIF withdrawal, passage 2. (*D*) Expression analysis of lineages and pluripotency-associated genes ([brown] mesoendoderm; [orange] ectoderm; [red] TE; [blue] endoderm; [purple] mesoderm; [green] pluripotency-associated) by RT-qPCR in control (gray) and Arid3a knockdown (white) ES cells following removal of LIF. (*E*) ES cell morphology upon OE of Arid3a. Arid3a-overexpressing cells were plated at clonal density, cultured for 5 d, and stained for AP. (*F*) Expression analysis of lineage markers by RT-qPCR in Arid3a OE-Pool (gray) and OE-High (white) cells. The data are plotted relative to the corresponding expression levels of control ES cells. All error bars depict standard deviations of biological triplicates. (*G*) Cell cycle comparisons of Arid3a-overexpressing cell lines (Arid3a OE-Pool and OE-High) with control ES and TS cells. The *Y*-axis is the distribution of cell cycle as measured by flow cytometry/DNA content.

normal culture conditions with LIF (Fig. 1C; Supplemental Fig. S1B). The results suggested that either Arid3a-deficient ES cells are less dependent on LIF, or the cells have impaired differentiation potential. However, after prolonged culture in the absence of LIF, we began to observe differentiated morphology of Arid3a-deficient cells (Supplemental Fig. S1D), suggesting that its loss delayed normal ES cell differentiation. Consistent with this, we observed delayed induction of lineage-specific marker genes such as Brachyury (mesoderm), Gata6 and Sox17 (endoderm), and Cdx2 and Gata3 (TE) as well as delayed down-regulation of ES cell core factors (Fig. 1D; Supplemental Fig. S1E). Notably, the most significantly affected genes upon knockdown of Arid3a were TE markers (Fig. 1D), suggesting that Arid3a may play a role in TE differentiation. We confirmed these results in an independent ES cell line (E14) and by using a shRNA targeted to the Arid3a 3′ untranslated region (UTR) (Supplemental Fig. S1F–I). The delayed differentiation observed upon knockdown of Arid3a was successfully rescued by OE of shRNA-resistant Arid3a (Supplemental Fig. S1H,I).

Induction of Arid3a in ES cells promotes TE differentiation

The results from knockdown of Arid3a suggested that the reciprocal action, OE of Arid3a, might promote ES cells to differentiate even in the presence of LIF. To examine this possibility, we generated a pool of Arid3a-overxpressing ES cells (Arid3a OE-Pool) and, from this, multiple clones with different levels of ectopic Arid3a expression (representative clones are shown in Supplemental Fig. S2A,B). Whereas clones expressing Arid3a modestly above endogenous levels (e.g., Arid3a OE-Low; approximately two-fold) displayed normal ES cell morphology (Supplemental Fig. S2A,B), clones with ~20-fold OE (e.g., Arid3a OE-High) displayed primarily differentiated phenotypes (flattened epithelial-like morphology) with weak AP activity (Fig. 1E,F). Arid3a OE-High cells exhibited significantly slower proliferative rates than normal ES cells (Supplemen-

tal Fig. S2C). Subsequent cell cycle analysis confirmed that Arid3a OE-High cells were reduced in actively proliferating (S-phase) populations and increased in G2/M-phase populations, which is similar to that of TS cells (Fig. 1G). Expression of a panel of multilineage markers revealed that many were activated by OE of Arid3a in ES cells, whereas pluripotency-associated gene levels were reduced (Fig. 1F; Supplemental Fig. S2D–F). TE lineage markers such as Cdx2, Gata3, Tcfap2c, and Hand1 showed particularly strong up-regulation upon OE of Arid3a in both J1 and E14 ES cells (Fig. 1F; Supplemental Fig. S2G–I), further indicating a role for Arid3a in TE lineage specification.

Global expression profiles of Arid3a-overexpressing ES cells are similar to those of TS cells

To better understand the global transcriptional impact of Arid3a perturbation in ES cells, we compared expression profiles of Arid3a knockdown and Arid3a OE-High cells with control ES cells using Affymetrix microarrays. We identified 1842 differentially expressed genes, with a cutoff threshold of 1.5-fold in at least one expression profile of Arid3a-overexpressing cell lines (Arid3a OE-High and OE-Pool). As expected from the data shown in Figure 1, A–D, gene expression changes upon knockdown of Arid3a were not significant compared with the changes upon OE of Arid3a (Fig. 2A).

A prior study revealed that ~50% reduction of Oct4, a master regulator of pluripotency, is sufficient to convert ES cells to TS-like cells (Niwa et al. 2000) that share many features with authentic TS cells derived from the TE layer of the early stage blastocyst. Since OE of Arid3a in ES cells significantly up-regulated many of the same TE lineage-specific markers (Fig. 1F) as knockdown of Oct4, we also compared the global expression profiles of Arid3a-overexpressing cell lines with those of TS-like cells derived by knockdown of Oct4 in ES cells. We observed highly similar gene expression patterns for Arid3a-overexpressing and Oct4 knockdown cells (Fig. 2A). Consistent with the propensity of Arid3a OE to promote TE lineage specification, the up-regulated genes upon OE of Arid3a were strongly enriched in gene ontology (GO) terms associated with placental and early embryonic development (Fig. 2B). On the other hand, the relatively fewer number of genes down-regulated upon OE of Arid3a were enriched in unrelated terms (e.g., RNA processing and cellular metabolic processes) (Supplemental Fig. S3A), further indicating that the cells are indeed differentiated, particularly toward the TE lineage.

Since ES cells are derived from the ICM of blastocysts, they are generally thought to have lost or suppressed the ability to generate TE and trophoblast lineages (Reubinoff et al. 2000). Nonetheless, several studies have reported that ES cells can directly *trans*-differentiate toward a TS-like cell fate (Niwa et al. 2005; Kuckenberg et al. 2010; Ralston et al. 2010). Therefore, we performed gene set enrichment analysis (GSEA) to further compare gene expression profiles of Arid3a-overexpressing cells with

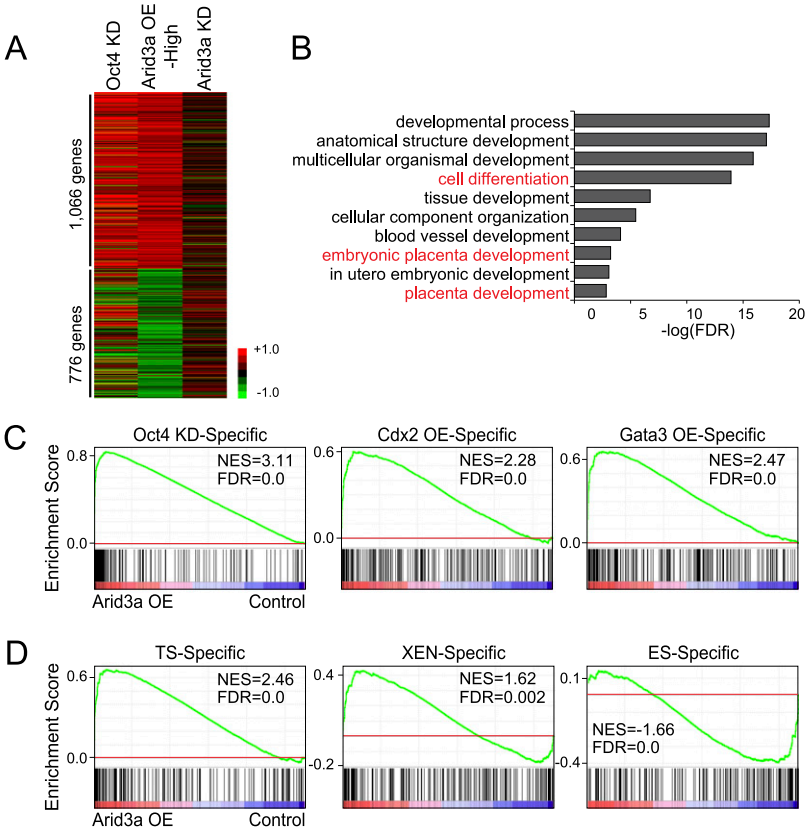

Figure 2. Expression profiles of Arid3a-overexpressing ES cells are highly similar to those of TS-like cells. (*A*) An unsupervised hierarchical clustering. A cutoff threshold of 1.5-fold from expression profile of Arid3a OE-High cells was applied. Expression profiles of Arid3a knockdown (KD) and Oct4 knockdown ES cells were plotted next to the clusters. (*B*) Significantly enriched terms (biological functions) of up-regulated genes upon OE of Arid3a shown in *A* by GO analysis. (*C*,*D*) GSEA using ordered gene expression levels from Arid3a-overexpressing cells over control ES cells (*X*-axis) with gene sets indicated. (*C*) Top 1% of up-regulated genes upon Oct4 knockdown (204 genes), Cdx2 OE (368 genes), and Gata3 OE (384 genes) in ES cells. (*D*) GSEA using TS cell-specific (313 genes), XEN cell-specific (227 genes), and ES cell-specific (218 genes) gene sets. (*C*,*D*) Normalized enrichment score (NES) and false discovery rate (FDR) are shown.

those of published TS-like cells generated by OE of Cdx2 or Gata3 (Ralston et al. 2010) or knockdown of Oct4 in ES cells. As shown in Figure 2C, each of the three gene sets (top 1% of genes up-regulated within each of the aforementioned profiles) showed highly significant enrichment in genes up-regulated upon OE of Arid3a in ES cells.

We carried out further GSEA with gene sets generated from the additional published expression data sets: TS cell-specific (TS cells vs. ES cells) (Ralston et al. 2010), extraembryonic endoderm (XEN) cell-specific (XEN cells vs. ES cells) (Ralston et al. 2010), and ES cell-specific (ES cells vs. differentiated ES cells) (Hailesellasse Sene et al. 2007). Consistent with our findings shown in Figures 1 and 2C, only TS cell-specific genes were strongly enriched among the up-regulated genes following OE of Arid3a in ES cells (Fig. 2D). While XEN cell-specific genes showed marginal enrichment, as predicted, ES cell-specific genes showed a negative correlation (Fig. 2D). Principal component analysis (PCA) indicated that Arid3a-overexpressing cells fall into a similar component with differentiated TS cells (days 10 and 14) (Supplemental Fig. S3B; Kidder and Palmer 2010). Furthermore, the expression levels of the top 50 most strongly expressed genes in TS cells and lineage markers tested in Figure 1F strongly overlapped with those in Arid3a-overexpressing ES cells (Supplemental Fig. S3C,D). Collectively, the findings indicate that OE of Arid3a in ES cells results in loss of ES cell identity and activation of TS cell-like global gene expression programs.

Induction of Arid3a in ES cells results in stable TS-like cells that are capable of further differentiation to trophoblast lineages

Although prior reports showed that OE of TE marker genes (e.g., Cdx2 and Gata3) in ES cells induces TE specification, not all of them are capable of producing stable, self-renewing TS-like cell lines (e.g., Gata3) (Niwa et al. 2005; Ralston et al. 2010). To examine whether induction of Arid3a in ES cells can lead to the establishment of stable and self-renewing TS-like cells, we adopted Arid3a OE-High cells to an established TS medium containing Fgf4 and heparin (Tanaka et al. 1998). After four passages, the cells displayed TS cell morphology; i.e., the majority of AP-negative cells gave rise to large and flattened cuboidal cells with distinctive boundaries (Fig. 3A). Moreover, these cells expressed multiple TE marker genes at levels similar to their counterparts in authentic TS cells derived from the TE of the blastocysts (Fig. 3B).

To test the potential of Arid3a-overexpressing cells to drive further TE differentiation, Arid3a-overexpressing TS-like cells were induced to differentiate by depleting Fgf4 and heparin from the TS culture medium. Within four to five passages, the cells appeared largely differentiated, with numerous giant cells present throughout the culture (Fig. 3C). These cells expressed markers for more specialized cells of the TE lineage, including Hand1, Id2, Dlx3, Wnt2, and Tpbpa (Fig. 3D), suggesting that Arid3a OE is not only sufficient for establishing the TE-like state but also may be required for further differentiation of the TE lineage.

Both Arid3a and Cdx2 are highly expressed in placenta and extraembryonic tissue such as TE (Supplemental Fig. S4A; Wheeler et al. 2003). However, analysis of public gene expression profiles (Kidder and Palmer 2010) indicated that Arid3a, but not Cdx2, is highly up-regulated in differentiated TS cells (Supplemental Fig. S4B). This observation prompted us to examine the effect of Arid3a OE on further differentiation of TS cells. Unlike control TS cells, TS cells with OE of Arid3a more closely resembled trophoblast giant cells (TGCs) even in the presence of Fgf4 and heparin (Fig. 3E). Accordingly, we observed up-regulation of transcripts (Gcm1, Hand1, Id2, Dlx3, Wnt2, and Tpbpa) preferentially expressed in TGCs and other more specialized trophoblastic lineages (Fig. 3F). Thus, in contrast to Cdx2, whose function is restricted to TE lineage specification, Arid3a regulates additional trophoblastic pathways beyond TE specification, as its OE in TS cells is sufficient to drive further trophoblastic differentiation.

Arid3a and Cdx2 act both independently and in concert to antagonize Oct4 and promote ES cells to TS cell trans*-differentiation*

To address whether Arid3a participates in the previously proposed Cdx2–Oct4 regulatory loop, we compared the consequences of Oct4 knockdown with double knockdown of Oct4 + Arid3a or Oct4 + Cdx2 in normal ES cell culture medium. As expected, control Oct4 knockdown cells displayed differentiated morphology (Fig. 3G) with strong up-regulation of TE markers, including both Cdx2 and Arid3a (data not shown). As with Oct4 + Cdx2 double knockdown, double knockdown of Oct4 + Arid3a led to significant reduction of the differentiated morphology with less induction of TE markers than control Oct4 knockdown cells (Fig. 3G,H). Immunostaining for Cdx2, Oct4, and Nanog confirmed these results (Supplemental Fig. S4C), indicating that Arid3a is at least in part involved in the Cdx2–Oct4 antagonistic regulatory loop.

To test whether the involvement of Arid3a in the Cdx2–Oct4 loop is through Cdx2 or independent of Cdx2, we performed Arid3a OE in combination with Cdx2 knockdown as well as Cdx2 OE in Arid3a knockdown cells. Cdx2 knockdown + Arid3a-overexpressing cells and Arid3a knockdown + Cdx2-overexpressing cells both showed differentiated morphology with induction of TE markers and repression of pluripotency genes (Supplemental Fig. S4D,E). Thus, Arid3a specifies TE not only through Cdx2 but also independent of Cdx2 and vice versa. That is, Arid3a and Cdx2 can induce TE-like gene expression programs in the absence of each other, although the effect is stronger when both are coexpressed.

Arid3a gain of function promotes incorporation of ES cells into the TE of developing embryos, whereas its loss of function leads to defective placentas

To examine the potential of Arid3a induction to establish the outside cell fate synonymous with in vivo commitment to the TE lineage, we marked Arid3a OE-driven TS-like cells with ZsGreen (Supplemental Fig. S5A) and

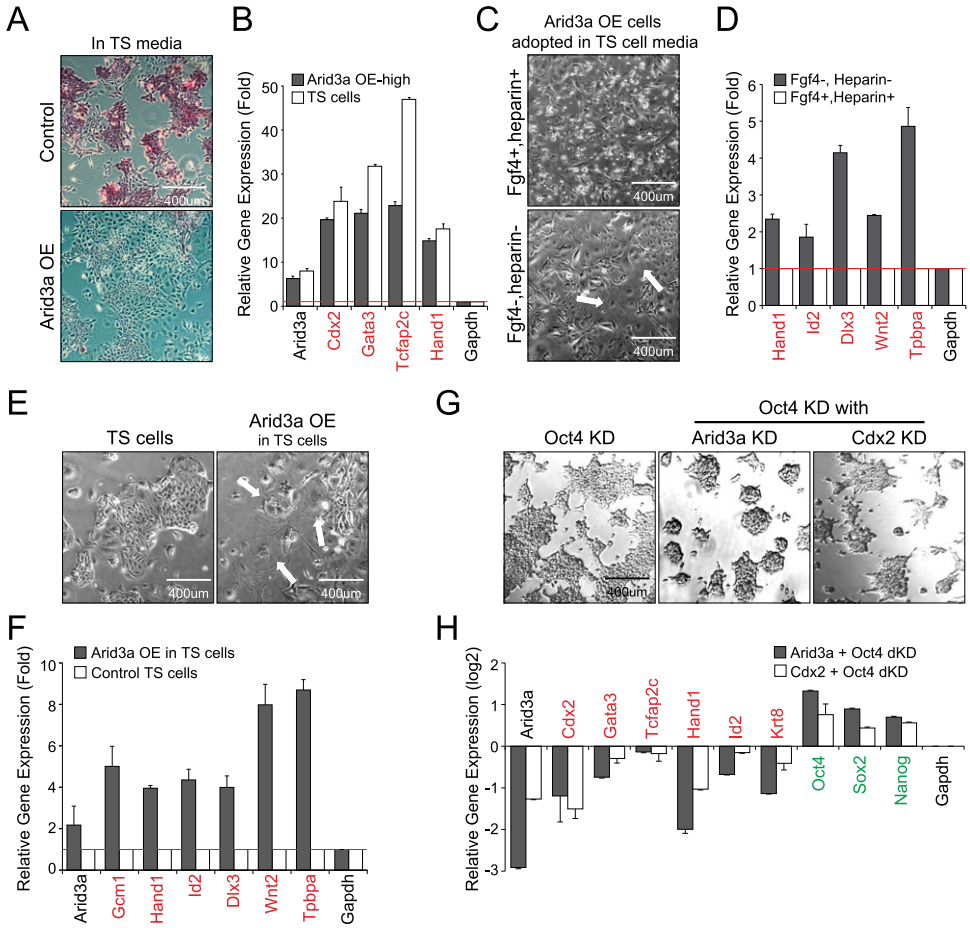

Figure 3. Induction of Arid3a converts ES cells to stable TS-like cells that can further differentiate to trophoblast lineages. (*A*) Cell morphologies of control ES and Arid3a-overexpressing cells in TS cell derivation medium containing Fgf4 and heparin. The cells were plated at clonal density, cultured for 5 d, and stained for AP. (*B*) Expression analysis of TE markers (red) by RT-qPCR in Arid3a-overexpressing cells in TS cell derivation medium (gray) and TS cells (white). The data are plotted relative to the corresponding expression levels of control ES cells grown in TS cell derivation medium. (*C*) Cell morphologies of Arid3a-overexpressing cells adapted to TS cell derivation medium (*top*) followed by removal of Fgf4 and heparin (*bottom*). Arrows indicate TGCs. (*D*) Arid3a OE in TS cell differentiation conditions promotes differentiation to more specialized cells of the TE lineage. Expression analysis of TE and trophoblast markers (red) as determined by RT-qPCR in Arid3a-overexpressing cells adapted to TS cell medium upon withdrawal of Fgf4 and heparin (gray). The data are plotted relative to corresponding expression levels of Arid3a-overexpressing cells adapted to TS cell culture medium (white). (*E*) Cell morphologies upon knockdown (KD) of Oct4 and double knockdown (dKD) of Oct4 + Arid3a or Oct4 + Cdx2 in ES cells under normal ES culture conditions. (*F*) Expressions of TE (red) and pluripotency-associated (green) genes as determined by RT-qPCR following the indicated knockdown perturbations (knockdown or double knockdown) in ES cells (LIF^+ conditions). The data are plotted relative to the corresponding expression levels in Oct4 knockdown cells. (*G*) Cell morphologies of control TS and Arid3a-overexpressing TS cells under TS cell derivation conditions. Arrows indicate TGCs. (*H*) Expression analysis of TE differentiation markers (red) upon OE of Arid3a in TS cells (gray) and in control TS cells (white) by RT-qPCR. Error bars depict standard deviations of biological triplicates.

injected them into four- to eight-cell stage mouse embryos, with Cdx2-ZsGreen-overexpressing TS-like cells as a positive control (Lu et al. 2008). At E3.5, control ES cells localized within the ICM, whereas Arid3a- and Cdx2-overexpressing cells were found exclusively within the TE layer (Fig. 4A). *Arid3a*$^{-/-}$-null (knockout)-derived ES cells (Webb et al. 2011) showed normal ES cell morphology (Supplemental Fig. S5B) but also failed to localize to the outer TE layer (Fig. 4A). These along with the above in vitro data indicate that gain of function of Arid3a is sufficient to not only direct TE fate but induce *trans*-differentiation of ES cells into TS-like cells with homing properties morphologically indistinguishable from bona fide TS cells.

While the cause of death of *Arid3a*-null embryos was assigned to failed erythropoiesis at E11.5 (Webb et al. 2011), potential placental defects were not examined. Genotypes of earlier developmental time points revealed loss of knockout Mendelian ratios as early as E8.5 (Supplemental Fig. S5C). In situ hybridization of *Arid3a*$^{+/+}$ embryos at E6.5 indicated strong Arid3a expression in the ectoplacental cone and extraembryonic ectoderm of

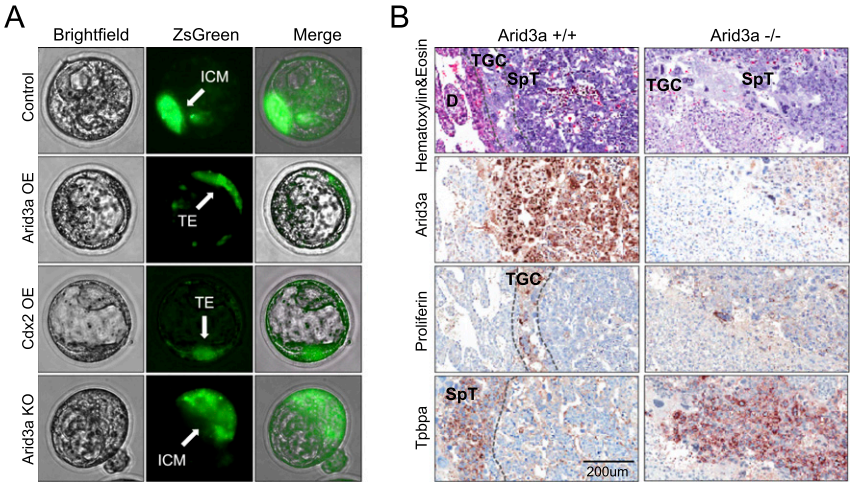

Figure 4. Arid3a OE promotes incorporation of ES cells into the TE of developing embryos, whereas its loss leads to defective placentas. (*A*) ZsGreen-Arid3a-overexpressing TS-like cells integrate into the TE layer of developing embryos, whereas *Arid3a*$^{-/-}$-null (knockout [KO]) ES cells remain within the ICM layer of ex vivo embryos. The four- to eight-cell stages of embryos injected with control ES cells and Cdx2-overexpressing cells served as negative and positive controls, respectively. (*B*) Placentas of E11.5 *Arid3a*$^{-/-}$ embryos are defective. IHC was performed with anti-proliferin, which marks TGCs, and anti-Tpbpa, which stains SpTs. (D) Deciduum. Anti-Arid3a IHC revealed high levels of Arid3a expression in *Arid3a*$^{+/+}$ TGCs and SpTs. The dotted lines denote the wild-type TGC and SpT expression domains that are grossly disorganized in the null placentas.

the chorion—sites at which multipotent TS cells reside (Supplemental Fig. 5D; Uy et al. 2002). Placental cell types that derive from these regions—TGCs and spongiotrophoblasts (SpTs)—strongly expressed Arid3a within their nuclei, as shown in E11.5 *Arid3a*$^{+/+}$ sections by immunohistochemistry (IHC) (Fig. 4B; Supplemental Fig. S5E,F). IHC of E11.5 sections of *Arid3a*$^{-/-}$ placentas revealed multiple abnormalities. These included (1) reduction and disorganization of TGCs and the TGC cell layer, with multiple TGCs aberrantly located in the SpT and labyrinth layers; (2) lack of an organized and compact SpT layer; (3) reduction in the number of fetal blood vessels in the labyrinth (particularly in the central region); and (4) reduction in the number of maternal blood spaces in the labyrinth (Fig. 4B; Supplemental Fig. S5F). Thus, Arid3a is a critical regulator for not only TE lineage maintenance and differentiation but also proper placenta development.

Nuclear localization of Arid3a is required for Oct4 repression and TE differentiation

That Arid3a undergoes CRM1-dependent nucleocytoplasmic shuttling in B lymphocytes and other somatic cell types (Kim and Tucker 2006) led us to test its localization in the blastocyst and prior to the first segregation by whole-mount embryo staining. In the compacted morula stage, Arid3a is expressed in all blastomeres, with localization primarily in the cytoplasm (Fig. 5A). At E.3.5 (early blastocyst), Arid3a localizes only within the cytoplasm of the ICM but begins to accumulate within the nucleus of the outer cells (Fig. 5B). Around E.4.5 (late blastocyst stage), Arid3a is highly localized in the outer cells of the TE (Fig. 5A).

We next examined Arid3a localization relative to Oct4 in normal ES cells, Arid3a-overexpressing cell lines, and TS cells by immunofluorescence. As shown in Figure 5C, Arid3a, in contrast to Oct4, localized primarily within the cytoplasm of ES and Arid3a OE-Low cells. However, the significantly increased levels of Arid3a in OE-High cells led to primarily nuclear localization (Fig. 5C). Notably, differentiated ES cells, which have an elevated level of endogenous Arid3a, also showed enhanced nuclear accumulation of Arid3a (Supplemental Fig. S6A), as did TS cells (Fig. 5D), which express >60-fold higher levels of Arid3a than ES cells (Supplemental Fig. S6B). These results indicated that Arid3a, when elevated to levels sufficient to initiate *trans*-differentiation of ES cells to TS-like cells (Figs. 1E, 3A), accumulates within the nucleus through either enhanced nuclear entry or reduced nuclear export.

Even though Arid3a resides primarily in the cytoplasm in normal or Arid3a OE-Low cells, we observed no evidence for Oct4 sequestration within the cytoplasm (Fig. 5C). Thus, partitioning of Arid3a and Oct4 into different subcellular compartments in ES cells may explain why Arid3a knockdown had no effect on ES cell self-renewal (Fig. 1A; Supplemental Fig. S1A). Instead, immunofluorescence detected an opposite shift in nuclear intensities of Arid3a and Oct4 on OE of Arid3a (Fig. 5C; Supplemental Fig. S6A). This was confirmed semiquantitatively in Western blots of whole-cell extracts; i.e., Oct4 was reduced ~50% relative to control ES cells (Fig. 5E). That Oct4 knockdown up-regulated Arid3a levels by approximately eightfold (Fig. 5E) further suggested that Arid3a and Oct4 may reciprocally repress one another.

Cytoplasmic-to-nuclear translocation of Tead4, in addition to gene activation of key members of the Hippo pathway, is required for TE specification (Nishioka et al. 2008). While mRNA and protein levels of Hippo pathway components were not significantly altered (Supplemental Fig. S6C,D), we observed enhanced nuclear accumulation of Tead4 in Arid3a OE-high cells relative to ES cells (Supplemental Fig. S6E). Thus, induction of nuclear Arid3a leads to differential Tead4 localization, potentially contributing to ES-to-TS cell *trans*-differentiation. Unlike Tead4, Yap1 remained primarily concentrated in the

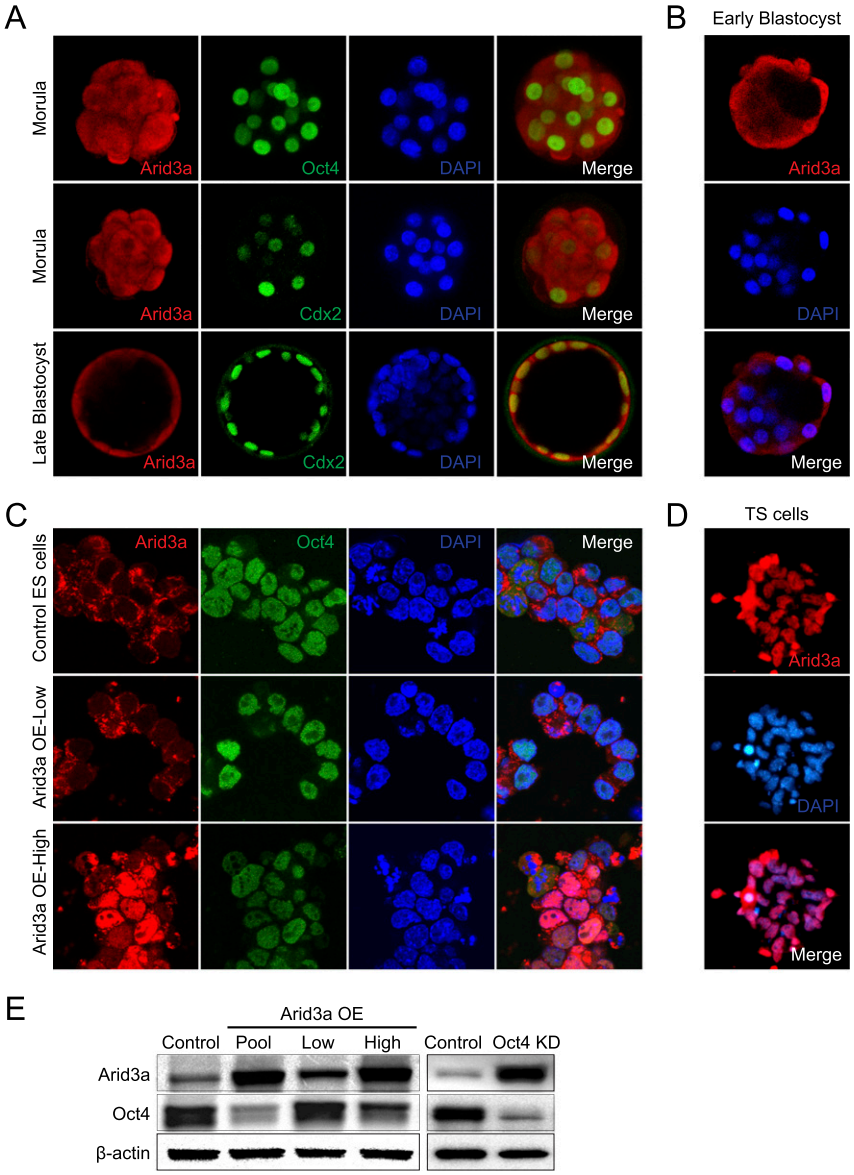

Figure 5. Nuclear localization of Arid3a is required for Oct4 repression and TE differentiation. (*A*,*B*) Whole-mount embryo staining of compacted morula, late blastocyst (*A*), and early blastocyst (*B*) stages with anti-Arid3a (red; Alexa 594), anti-Oct4 (green; Alexa 488), anti-Cdx2 (green; Alexa 488), and DAPI (blue). Arid3a localizes within all blastomeres of the compacted morula and primarily within the outer cells of TE in blastocyst. (*C*) Immunofluorescence images of control ES, Arid3a OE-Low, and Arid3a OE-High cells. All cells were stained with directly conjugated anti-Arid3a (red; Alexa 594) and anti-Oct4 (green; Alexa 488) as well as DAPI (blue). Arid3a is primarily cytoplasmic in ES or Arid3a OE-Low cells but shuttles to the nuclei of Arid3a OE-High ES cells, resulting in reduced levels of nuclear Oct4. (*D*) Immunofluorescence images of TS cells stained for endogenous Arid3a (red; Alexa 594) and DAPI (blue). (*E*) Western blotting showing protein levels of Arid3a and Oct4 following Arid3a OE or Oct4 knockdown (KD) in ES cells. β-Actin was the loading control.

nucleus of ES, TS, and Arid3a-overexpressing cells (Supplemental Fig. S6E).

Target occupancy of Arid3a correlates with Arid3a-mediated gene expression

Arid3a and Oct4 reciprocally regulate transcript levels of many lineage-specific and pluripotency-associated genes (Fig. 2A). This along with the above results (Fig. 5) raised the possibility that Arid3a and Oct4 may share common target genes. We first mapped the global target loci of Arid3a using in vivo biotinylation-mediated chromatin immunoprecipitation (bioChIP) (Kim et al. 2009) followed by massively parallel sequencing. Higher levels of Arid3a OE, as expected from its enhanced nuclear localization (Fig. 5), increased the overall occupancy signals of Arid3a (Fig. 6A). The target loci of Arid3a were primarily distributed within intergenic (~42%) and promoters (~31%), suggesting that Arid3a regulates both proximal and distal regulatory elements (Fig. 6B). We then compared the target occupancy of Arid3a with the gene expression profiles of Arid3a-overexpressing cells using a moving window average (window size, 250; bin size, 1). As shown in Figure 6C, a large number of genes up-regulated or down-regulated upon OE of Arid3a are direct transcriptional targets of Arid3a (Fig. 6C; Supplemental Fig. S7A,B). Thus, during Arid3a-mediated TE *trans*-differentiation, Arid3a acts as both an activator and a repressor of target gene transcription.

Arid3a directly activates TE markers and directly represses pluripotency factors during ES-to-TS cell trans*-differentiation*

Recent target mapping of various TFs in ES cells revealed that clusters of relatively high numbers of TFs act together to regulate their common targets (Kim et al.

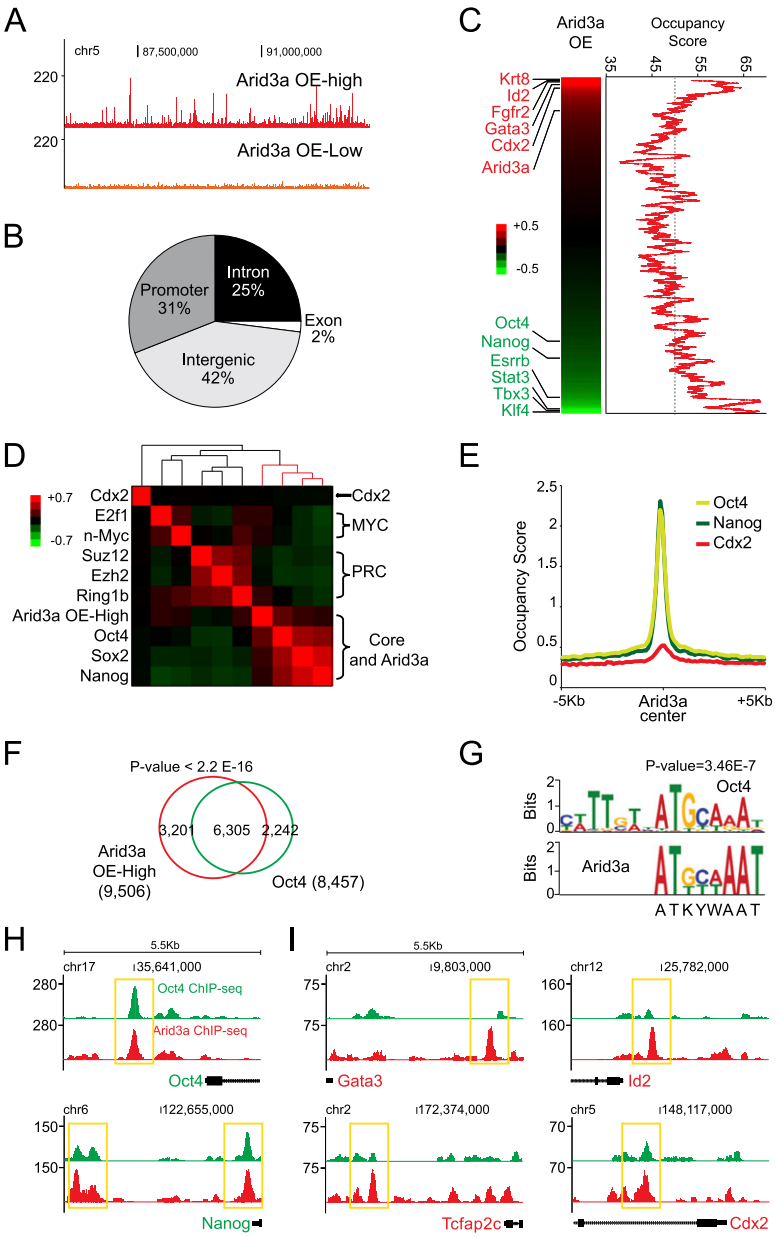

Figure 6. Arid3a and Oct4 occupy highly similar target loci. (*A*) A snapshot of a random locus on chromosome 5 illustrating that Arid3a ChIP-seq occupancy signals derived from Arid3a OE-High ES cells are stronger than those of Arid3a OE-Low cells. (*B*) Pie chart presenting the distribution of Arid3a peaks. Promoters indicate regions within ±2 kb from the transcription start sites (TSSs). Intergenic depicts regions other than promoters, exons, or introns. (*C*) A heat map representation of the expression profile of Arid3a-overexpressing cells with representative gene names ([red] TE-specific genes; [green] pluripotency-associated genes). Genes were ordered according to gene expression levels in Arid3a-overexpressing cells relative to control ES cells. Moving average (window size, 250; bin size, 1) was plotted to corresponding Arid3a occupancy signals. (*D*) Target correlation map of the indicated TFs illustrating that Arid3a target loci overlap with those of core TFs. (*E*) Binding positions of Oct4 (yellow), Nanog (green), and Cdx2 (red) relative to the center of corresponding Arid3a target loci. (*F*) Venn diagram showing that the majority of Oct4 and Arid3a target genes overlap. Numbers indicate target genes of Arid3a (red circle) and Oct4 (green circle). (*G*) Motif analysis of Arid3a and Oct4 target loci indicates that the prototypical octamer motif is the most highly enriched DNA-binding site for both TFs. (*H*,*I*) Snapshots of ChIP-seq signal tracts of Oct4 (green) and Arid3a (red) at the regulatory regions of pluripotency-associated genes (*H*) and TE markers (*I*).

2008). To gain further insight into Arid3a-mediated global gene regulation, we compared its target occupancy in Arid3a OE-High ES cells with publicly available ES cell ChIP-seq (ChIP combined with deep sequencing) data for the following factors: pluripotency-associated TFs (Oct4, Sox2, and Nanog), key components of Polycomb-repressive complex (Ezh2, Suz12, and Ring1b), Myc-related (n-Myc and E2f1), and the TE master regulator Cdx2 (Fig. 6D). Although Arid3a and Cdx2 have similar consequences on ES-to-TS cell *trans*-differentiation, we found very low accordance in their target sets (Fig. 6D,E; Supplemental Fig. S7C), indicating that their underlying TE regulatory mechanisms must differ. Instead, Arid3a target loci strongly overlapped with those of pluripotency-associated factors (Fig. 6D–F; Supplemental Fig. S7C), and Arid3a target genes are highly enriched in the previously defined ES cell core module (Supplemental Fig. S7D; Kim et al. 2010). Notably, we observed strong enrichment of the Oct4 DNA-binding motif in Arid3a target loci with the perfectly conserved core octamer sequence (ATGCAAAT) (Fig. 6G). Accordingly, Arid3a and Oct4 occupied the same regulatory regions of numerous pluripotency-associated genes, including *Oct4* itself and *Nanog*, whereas TE-specific genes, including *Cdx2*, *Gata3*, *Id2*, and *Tcfap2c*, were singularly occupied by Arid3a (Figure 6H,I). Gene ontogeny analyses predicted highly significant enrichment of Arid3a targets in signatures associated with blastocyst formation, trophectodermal cell differentiation, and early embryogenesis (Supplemental Fig. S7E,F). We conclude that, in general,

the gene targets shared by Arid3a and Oct4 are repressed, whereas the targets occupied by only Arid3a are activated upon induction of Arid3a in ES cells.

Arid3a represses pluripotency-associated genes by recruiting HDACs

HDACs have been implicated in numerous transcriptional repression and chromatin remodeling contexts as well as in silencing of cell fate decisions (Dovey et al. 2010). Recent reports suggested that HDACs are associated with ES cell core factors in a complex termed "NODE" for Nanog and Oct4-associated deacetylases (Liang et al. 2008). Furthermore, a significant number of pluripotency-associated TFs share their targets with HDACs (Whyte et al. 2012). Thus, we reasoned that HDACs may distinguish Arid3a-mediated repression from Arid3a-mediated activation (Fig. 6H,I). Consistent with this hypothesis, we observed strong Arid3a–HDAC1/2 coimmunoprecipitation (co-IP) in Arid3a OE-High cells (Fig. 7A).

Since the levels of HDAC1 and HDAC2 were not elevated by Arid3a OE in ES cells (data not shown), we used HDAC1 ChIP to determine whether the target occupancies of HDAC1 are altered upon OE of Arid3a. As shown in Figure 7B and Supplemental Figure S8, HDAC1 occupied regulatory elements of pluripotency-associated genes more strongly following Arid3a OE than in control ES cells, whereas only modest changes were observed in regulatory elements of TE-specific genes. In contrast, activation-associated histone acetylation marks (AcH3 and AcH4) were significantly enriched at the regulatory regions of TE-specific marker genes, whereas weaker signals were associated with pluripotency-associated genes (Fig. 7C). These data suggested that the repression of pluripotency-related genes in Arid3a-overexpressing cells is at least in part mediated by the activity of HDAC1 and Arid3a, whereas histone acetyltransferases (HATs) are recruited to TE-specific regulatory elements with Arid3a. In further support of this notion, target genes co-occupied by both HDAC1 and Arid3a, many of which are ES cell-specific (Fig. 7F, top), are strongly repressed upon induction of Arid3a (Fig. 7D,F). Conversely, regulatory elements of TE-specific genes that are up-regulated upon OE of Arid3a were not co-occupied by HDAC1 and Arid3a (Fig. 7E). Unique targets of HDAC1 were not restricted to either TS cell- or ES cell-specific genes (Fig. 7F, bottom). These data along with the co-IP results (Fig. 7A) indicate that the repression of pluripotency-associated genes upon OE of Arid3a is mediated by selective recruitment of HDAC1 onto their common *cis*-regulatory elements.

Discussion

Here we identify Arid3a as a central transcriptional regulator of TE lineage commitment and differentiation. Arid3a is highly expressed in vitro in nuclei of TE and TS cells as well in vivo in outer cells of early blastocyst and TE-derived placental lineages. OE of Arid3a is sufficient to *trans*-differentiate ES cells into TS-like cells in vitro. When transplanted into developing mouse blastocysts ex vivo, Arid3a-driven TS-like cells integrate into the TE layer of developing embryos. The induction of Arid3a in TS cells leads to further differentiation of TS cells to more specialized trophoblastic lineages—a fate not executed by Cdx2. Arid3a acts both directly upstream and independently of Cdx2 to promote TE pathways while directly repressing Oct4-dependent pluripotency pathways. We provide evidence that selective TE versus ES gene regulation is mediated epigenetically via differential HDAC recruitment.

Trans-differentiation of ES cells toward TE lineage via OE of a single TF was previously reported for Cdx2 and Gata3 (Niwa et al. 2005; Ralston et al. 2010). Although our data on Arid3a show similar consequences on TE fate specification, we found that Arid3a and Cdx2 do not appear to share similar regulatory mechanisms. While the prior work using Cdx2-inducible ES cells showed exclusive target occupancy of Cdx2 on TE lineage-specific genes (Nishiyama et al. 2009), our genome-wide mapping revealed that Arid3a directly binds to the regulatory elements of both TE-specific factors (including *Cdx2, Gata3, Tcfap2c,* and *Id2*) and pluripotency-associated genes (such as *Oct4* and *Nanog*) during *trans*-differentiation (Fig. 6). This differential target gene occupancy between Cdx2 and Arid3a is consistent with their phenotypic dissimilarity found during the differentiation of TS cells into more specialized trophoblast cells (Fig. 3), further indicating the existence of multiple subregulatory networks responsible for TE lineage specification or differentiation.

Notably, we found that Arid3a directly occupies the regulatory elements of Cdx2 (Fig. 6), suggesting that, at least in certain contexts, Arid3a is an upstream regulator of this TE "master" regulator. On the other hand, Cdx2 and Arid3a also operate in parallel pathways to achieve TE *trans*-differentiation, as shown by reciprocal knockdown and OE analyses of Figure 3. It will be of great interest to identify additional key regulators of TE lineage specification and elucidate how these regulators are intertwined in combination with other coregulators to coordinate downstream gene expression programs during early cell fate decision and eventually placenta development.

We show TE segregation both in vivo and in cultured ES cells under natural or ectopically induced high levels of Arid3a, which the subcellular localization of Arid3a correlates strongly with execution of TE fate. Arid3a largely resides in the cytoplasm of early blastomeres and the ICM but, by E4.5, undergoes translocation to nuclei of the outer TE cells (Fig. 5). Similarly, its translocation from self-renewing ES cell cytoplasm to the nucleus is required to repress the TE antagonist Oct4 to levels sufficient to promote ES-to-TE *trans*-differentiation and consistent with prior studies (Niwa et al. 2000). Further supporting our hypothesis, both TS cells and Arid3a OE-derived TS-like cells as well as placental TGCs and SpTs displayed primarily nuclear localization of Arid3a (Figs. 4, 5). Previous studies showed that Arid3a undergoes CRM1-dependent nucleocytoplasmic shuttling

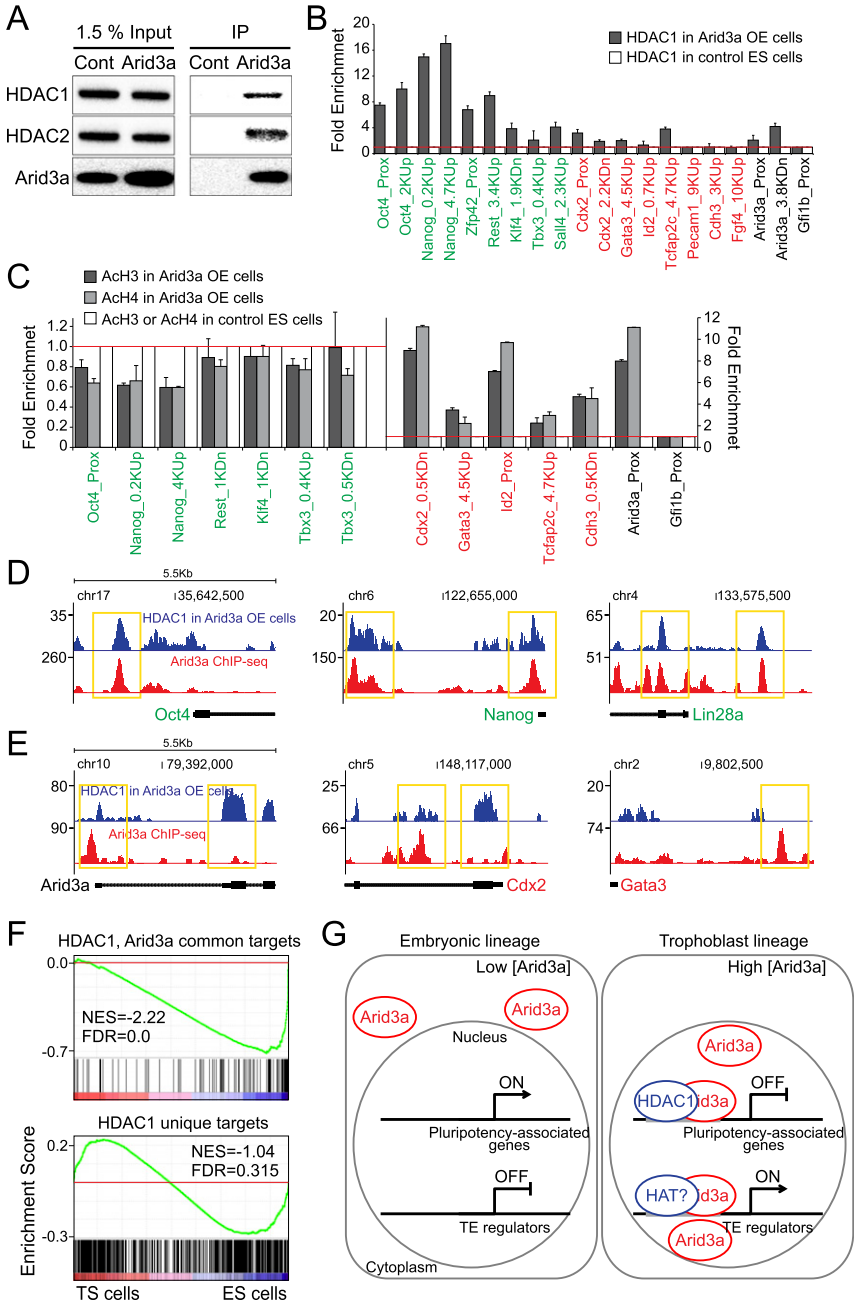

Figure 7. Arid3a recruits HDACs onto loci of pluripotency-associated genes. (*A*) Immunoprecipitation (IP) of Arid3a complexes from control ES cells (Cont) or Arid3a OE-High ES cells (Arid3a) followed by Western blotting with antibodies against HDAC1, HDAC2, and Arid3a. (*B*) Fold enrichments of HDAC1 binding to the regulatory regions of pluripotency-associated genes (red), lineage markers (green), and Arid3a (black) as determined by ChIP-qPCR in Arid3a-overexpressing cells (gray) relative to control ES cells (white). (*C*) Fold enrichments of AcH3 (gray) and AcH4 (light gray) marks at the regulatory regions of pluripotency-associated genes (red), lineage markers (green), and Arid3a (black) as determined by ChIP-qPCR in Arid3a-overexpressing cells relative to control ES cells (white). (*B*,*C*) The proximal promoter of Gfi1b served as a control (black; *X*-axis). Error bars depict standard deviations of biological triplicates. (Prox) Regions proximal to the TSS; (Up) regions upstream of the TSS; (Dn) regions downstream from the TSS. (*D*,*E*) Snapshots of ChIP-seq signal tracts of HDAC1 (blue) and Arid3a (red) at the regulatory regions of pluripotency-associated genes (*D*) and TE-associated genes (*E*). (*F*) GSEA using gene sets of targets in common between HDAC1 and Arid3a or unique to HDAC1. Genes ordered according to gene expression levels in TS cells relative to ES cells (*X*-axis). Normalized enrichment score (NES) and false discovery rate (FDR) are shown. (*G*) Embryonic versus trophoblastic lineage choice depends on differential nuclear import and HDAC association of Arid3a.

in somatic cell types, but the underlying mechanism remains unknown (Kim and Tucker 2006). A similar mechanism was shown to activate Tead4, the well-defined Hippo pathway TF essential for TE specification (Nishioka et al. 2008). Accordingly, we observed Tead4 translocation correlated with Arid3a nuclear levels (Fig. 5). An important subject of future study will be to determine how the nuclear localization of Arid3a is post-translationally regulated and the consequences on its distinct transcriptional programs in ES and TS cells.

We observed a strong correlation between Arid3a-bound target genes with transcripts deregulated upon Arid3a OE. The general pattern was that upon Arid3a OE, TE factors were activated, and pluripotent factors were repressed. A central question raised by our integrative DNA-binding and global gene expression analysis was how Arid3a functions as both an activator and a repressor depending on its target genes. The first hint was our finding that Arid3a interacts with HDAC1 and HDAC2 at the protein level (Fig. 7). HDACs generally convey repressive function in somatic cells, particularly in the context of the NuRD complex. However, recent studies indicate that HDACs are also bound to active chromatin in both ES and TS cells (Kidder and Palmer 2012). In ES cells, HDAC1 associates with regulatory regions of key TFs implicated in the maintenance of ES

cell self-renewal (such as *Oct4*, *Sox2*, and *Nanog*), whereas, in TS cells, HDAC1 binds to crucial TE genes (including *Cdx2*, *Elf5*, and *Eomes*) (Kidder and Palmer 2012). Our HDAC1 ChIP followed by quantitative PCR (qPCR) analysis indicated that Arid3a OE promotes stronger occupancy of HDAC1 onto the regulatory elements of pluripotency-associated genes without significant occupancy changes at the regulatory elements of TE-specific genes. Importantly, a high level of Arid3a–HDAC1 co-occupancy is observed at pluripotency-associated loci in Arid3a-overexpressing TS-like cells. Perhaps this Arid3a–HDAC1 interaction alters the activity/specificity of HDAC1, leading to deacetylation of pluripotency-associated nucleosomal histone tails (Fig. 7). Thus, differential co-occupancy of HDAC1 and Arid3a may be responsible for the repressive role of Arid3a. Our results in Figure 7C additionally suggest putative associations of Arid3a and HAT for the activation of TE-specific genes.

While Arid3a can phenocopy, if not surpass, Cdx2 in executing ES-to-TE *trans*-differentiation in cultured cells, there is a critical difference in vivo. Cdx2 is critical for the first cell fate commitment of the TE, as *Cdx2*$^{-/-}$ embryos fail to implant (Strumpf et al. 2005). However, while fetal death was observed as early as E8.5 (Supplemental Fig. S5C), the majority of *Arid3a*-null embryos can implant and develop to as late as E11.5 (Webb et al. 2011), albeit with gross defects in placental cellularity and architecture, including expression and organization of the direct descendants of TE, TGCs, and SpTs (Fig. 4; Uy et al. 2002). However, in the in vitro context, Arid3a can directly activate *Cdx2* and indirectly activate an arm of the Hippo pathway (shown to be upstream of Cdx2 by inducing Tead4 nuclear localization)—events associated previously with the specification phase of the first cell fate. Perhaps, in vitro, the distinction between specification and commitment is less strict than in vivo, where these steps are readily distinguished by preimplantation and post-implantation. We are currently examining *Arid3a*$^{-/-}$ preimplantation embryos to better resolve this issue.

Although not entirely analogous, many of these processes in mice are conserved in human placenta development. A notable exception and in support of the possibility that Arid3a acts in parallel with Cdx2 is that the reciprocal Cdx2–Oct4 expression patterns observed in mice are not conserved in humans (Hay et al. 2004). Further consistent with defects in the *Arid3a*$^{-/-}$ placentas, disruption of the migration of differentiating TGCs can result in poorly formed vessels that lead to vascular insufficiency of the placenta and fetus, which in turn may result in preeclampsia (Red-Horse et al. 2004). Expression profiling of human chorionic trophoblast progenitor cells and primary villous trophoblasts identified Arid3a as highly expressed in these lineages (Genbacev et al. 2011). Human TGCs, which highly express Arid3a (Genbacev et al. 2011), are the first cell type to terminally differentiate during embryogenesis and are of vital importance for implantation and modulation of the post-implantation placenta (Red-Horse et al. 2004). These findings point to potential Arid3a involvement in human placental fate and maintenance and suggest that it will be extremely informative to determine Arid3a function in both normal and preeclamptic placenta.

Materials and methods

Cell culture and stable cell lines

Mouse J1 ES cells were maintained in DMEM (Dulbecco's modified Eagle's medium) supplemented with 18% fetal bovine serum (FBS), 2 mM L-glutamine, 100 μM nonessential amino acid, nucleoside mix (100× stock; Sigma), 100 μM β-mercaptoethanol, 1000 U/mL recombinant LIF (Chemicon), and 50 U/mL penicillin/streptomycin. ES cells were cultured in 0.1% gelatin-coated dishes. Mouse TS cells were maintained at a ratio of 3:7 of TS medium to MEF-conditioned TS medium with 25 ng/mL Fgf4 and 1 μg/mL heparin. The TS medium was RPMI 1640 (Gibco) supplemented with 20% FBS, 100 μM β-mercaptoethanol, 2 mM L-glutamine, 1 mM sodium pyruvate, 50 U/mL penicillin, and 50 mg/mL streptomycin. The MEF-conditioned medium was TS medium conditioned by MEF cells. Mitomycin-treated MEF cells were cultured in TS medium for 3 d. The medium was collected every 3 d for three times. 293T cells were maintained in DMEM supplemented with 10% FBS, 2 mM L-glutamine, and 50 U/mL penicillin/streptomycin. All cells were incubated at 37°C and 5% CO_2.

Lentiviral production and infection

293T cells were plated at ~6×10^6 cells per 100-mm dish and incubated overnight. Cells were transfected with 6 μg of pLKO.1 shRNA vector (Sigma) (Supplemental Table. S3) with 4 μg of pCMV-Δ8.9 and 2 μg of VSVG helper plasmids using Fugene (Promega), according to the manufacturer's instructions. After 15 h, 293T medium was replaced with ES medium. Two days following transfection, the supernatants containing viral particles were collected and filtered through 0.45-μm pore size cellulose acetate filters. The cells, which would be infected, were plated at ~1×10^6 cells per six-well plate with virus-containing supernatant supplemented with polybrene (Millipore).

Quantitative gene expression analysis

Total RNA was isolated from cultured cells using the RNeasy plus minikit (Qiagen). cDNA synthesis was performed with qScript cDNA supermix (Quanta). RT-qPCRs were performed using PerfeCTa SYBR Green FastMix (Quanta) with 1 μL of 20×-diluted cDNA generated from 500 ng of total RNA. RT-qPCR primers were designed to amplify the junction between two exons using primer 3 (Koressaar and Remm 2007). ChIP-qPCR primers were designed to amplify ~100-base-pair (bp) regions centered on the putative binding sites. Primer sequences for qPCR are listed in Supplemental Table. S3. CT values were normalized against Gapdh for gene expression and compared with Gfi1b_proximal promoter binding (negative control) for ChIP enrichment.

Microarrays and gene expression analysis

Affymetrix GeneChip mouse genome 430A 2.0 arrays were used for gene expression profiles. cDNA synthesis, labeling, hybridization, washing, and scanning were performed by the Microarray Core Facility at the Dana Farber Cancer Institutes (DFCI). Expression data were normalized using a robust multiple array (RMA).

ChIP-seq

ChIP assays were done with ES cell lines expressing BirA only (reference) or both BirA and biotin-tagged proteins (samples) as previously described (Kim et al. 2008) using streptavidin magnetic particles (Roche). ChIP-seq libraries were generated using ChIP-seq library prep kits (New England Biolabs) according to the manufacturer's instructions. ChIP-seq libraries were sequenced using an Illumina HiSeq 2500 at the Genomic Sequencing and Analysis Facility (GSAF) of The University of Texas at Austin. Raw and processed microarrays and ChIP-seq data have been deposited at the public server Gene Expression Omnibus (GEO) under accession number GSE56877.

Immunofluorescence

Glass coverslips were affixed to the bottom of six-well plates followed by 0.1% gelatin coating. The cells were plated at high density and grown for 1–3 d at 37°C. Slides were incubated in 4% paraformaldehyde (in PBS) for 15 min at room temperature followed by 5% Triton X-100 (in PBS) incubation for 10 min at room temperature. Slides were then incubated in blocking solution (3% BSA + 1% normal horse serum in PBS) for 1 h at room temperature, primary antibody solution (1:200 dilution) for 1 h at room temperature, and secondary antibody conjugated to Alexa Fluor 594 or Alexa Flour 488 dyes (1:1000 dilution) for 1 h in the dark at room temperature. Last, the glass coverslips were dried, affixed to slides using mounting solution, and imaged on a Zeiss 710 laser scanning confocal and structured illumination microscope.

Embryo chimeras

Host embryos were obtained from B6D2F1 mice and collected at the two-cell stage. Approximately 10 ES, Arid3a-overexpressing, or Cdx2-overexpressing cells expressing ZsGreen (pEF1α-IRES-ZsGreen1, Clontech) were injected into four- to eight-cell stage embryos. After injection, the embryos were cultured in vitro in KSOM+AA (Millipore). Images were collected at E3.5.

Acknowledgments

We thank Dr. Janet Rossant (University of Toronto) and Dr. Guang Hu (National Institutes of Health [NIH]/National Institute of Environmental Health Sciences [NIEHS]) for providing TS cells; Jin Xiang Ren (University of Texas), June Harris (University of Texas), and Dr. Yuko Fujiwara (Harvard Medical School) for help with embryo chimeras; Dr. Donna Kusewitt (University of Texas MD Anderson Smithville) and University of Texas MD Anderson Smithville histology core for help with placenta IHC; Dr. Andrew Woo for critical reading of the manuscript; and the Genome Sequencing and Analysis Facilities (University of Texas) for ChIP sample processing and next-generation sequencing. This work was supported by awards from the NIH (R00GM088384) and the Cancer Prevention Research Institute of Texas (Cancer Prevention Research Institute of Texas [CPRIT], R1106) to J.K., and from the NIH (R01CA31534), CPRIT (RP120459), and the Marie Betzner Morrow Centennial Endowment to H.O.T. J.K. is a CPRIT Scholar.

References

Auman HJ, Nottoli T, Lakiza O, Winger Q, Donaldson S, Williams T. 2002. Transcription factor AP-2γ is essential in the extra-embryonic lineages for early postimplantation development. *Development* **129:** 2733–2747.

Chawengsaksophak K, James R, Hammond VE, Kontgen F, Beck F. 1997. Homeosis and intestinal tumours in Cdx2 mutant mice. *Nature* **386:** 84–87.

Dietrich JE, Hiiragi T. 2007. Stochastic patterning in the mouse pre-implantation embryo. *Development* **134:** 4219–4231.

Dovey OM, Foster CT, Cowley SM. 2010. Histone deacetylase 1 (HDAC1), but not HDAC2, controls embryonic stem cell differentiation. *Proc Natl Acad Sci* **107:** 8242–8247.

Evans MJ, Kaufman MH. 1981. Establishment in culture of pluripotential cells from mouse embryos. *Nature* **292:** 154–156.

Genbacev O, Donne M, Kapidzic M, Gormley M, Lamb J, Gilmore J, Larocque N, Goldfien G, Zdravkovic T, McMaster MT, et al. 2011. Establishment of human trophoblast progenitor cell lines from the chorion. *Stem Cells* **29:** 1427–1436.

Hailesellasse Sene K, Porter CJ, Palidwor G, Perez-Iratxeta C, Muro EM, Campbell PA, Rudnicki MA, Andrade-Navarro MA. 2007. Gene function in early mouse embryonic stem cell differentiation. *BMC Genomics* **8:** 85.

Hay DC, Sutherland L, Clark J, Burdon T. 2004. Oct-4 knockdown induces similar patterns of endoderm and trophoblast differentiation markers in human and mouse embryonic stem cells. *Stem Cells* **22:** 225–235.

Herrscher RF, Kaplan MH, Lelsz DL, Das C, Scheuermann R, Tucker PW. 1995. The immunoglobulin heavy-chain matrix-associating regions are bound by Bright: a B cell-specific *trans*-activator that describes a new DNA-binding protein family. *Genes Dev* **9:** 3067–3082.

Kidder BL, Palmer S. 2010. Examination of transcriptional networks reveals an important role for TCFAP2C, SMARCA4, and EOMES in trophoblast stem cell maintenance. *Genome Res* **20:** 458–472.

Kidder BL, Palmer S. 2012. HDAC1 regulates pluripotency and lineage specific transcriptional networks in embryonic and trophoblast stem cells. *Nucleic Acids Res* **40:** 2925–2939.

Kim D, Tucker PW. 2006. A regulated nucleocytoplasmic shuttle contributes to Bright's function as a transcriptional activator of immunoglobulin genes. *Mol Cell Biol* **26:** 2187–2201.

Kim J, Chu J, Shen X, Wang J, Orkin SH. 2008. An extended transcriptional network for pluripotency of embryonic stem cells. *Cell* **132:** 1049–1061.

Kim J, Cantor AB, Orkin SH, Wang J. 2009. Use of in vivo biotinylation to study protein-protein and protein-DNA interactions in mouse embryonic stem cells. *Nat Protoc* **4:** 506–517.

Kim J, Woo AJ, Chu J, Snow JW, Fujiwara Y, Kim CG, Cantor AB, Orkin SH. 2010. A Myc network accounts for similarities between embryonic stem and cancer cell transcription programs. *Cell* **143:** 313–324.

Koressaar T, Remm M. 2007. Enhancements and modifications of primer design program Primer3. *Bioinformatics* **23:** 1289–1291.

Kuckenberg P, Buhl S, Woynecki T, van Furden B, Tolkunova E, Seiffe F, Moser M, Tomilin A, Winterhager E, Schorle H. 2010. The transcription factor TCFAP2C/AP-2γ cooperates with CDX2 to maintain trophectoderm formation. *Mol Cell Biol* **30:** 3310–3320.

Liang J, Wan M, Zhang Y, Gu P, Xin H, Jung SY, Qin J, Wong J, Cooney AJ, Liu D, et al. 2008. Nanog and Oct4 associate with unique transcriptional repression complexes in embryonic stem cells. *Nat Cell Biol* **10:** 731–739.

Lu CW, Yabuuchi A, Chen L, Viswanathan S, Kim K, Daley GQ. 2008. Ras-MAPK signaling promotes trophectoderm formation from embryonic stem cells and mouse embryos. *Nat Genet* **40:** 921–926.

Nichols J, Zevnik B, Anastassiadis K, Niwa H, Klewe-Nebenius D, Chambers I, Scholer H, Smith A. 1998. Formation of pluripotent stem cells in the mammalian embryo depends on the POU transcription factor Oct4. *Cell* **95:** 379–391.

Nishioka N, Yamamoto S, Kiyonari H, Sato H, Sawada A, Ota M, Nakao K, Sasaki H. 2008. Tead4 is required for specification of trophectoderm in pre-implantation mouse embryos. *Mech Dev* **125:** 270–283.

Nishioka N, Inoue K, Adachi K, Kiyonari H, Ota M, Ralston A, Yabuta N, Hirahara S, Stephenson RO, Ogonuki N, et al. 2009. The Hippo signaling pathway components Lats and Yap pattern Tead4 activity to distinguish mouse trophectoderm from inner cell mass. *Dev Cell* **16:** 398–410.

Nishiyama A, Xin L, Sharov AA, Thomas M, Mowrer G, Meyers E, Piao Y, Mehta S, Yee S, Nakatake Y, et al. 2009. Uncovering early response of gene regulatory networks in ESCs by systematic induction of transcription factors. *Cell Stem Cell* **5:** 420–433.

Niwa H. 2007. How is pluripotency determined and maintained? *Development* **134:** 635–646.

Niwa H, Miyazaki J, Smith AG. 2000. Quantitative expression of Oct-3/4 defines differentiation, dedifferentiation or self-renewal of ES cells. *Nat Genet* **24:** 372–376.

Niwa H, Toyooka Y, Shimosato D, Strumpf D, Takahashi K, Yagi R, Rossant J. 2005. Interaction between Oct3/4 and Cdx2 determines trophectoderm differentiation. *Cell* **123:** 917–929.

Pfeffer PL, Pearton DJ. 2012. Trophoblast development. *Reproduction* **143:** 231–246.

Popowski M, Templeton TD, Lee BK, Rhee C, Li H, Miner C, Dekker JD, Orlanski S, Bergman Y, Iyer VR, et al. 2014. Bright/Arid3A acts as a barrier to somatic cell reprogramming through direct regulation of Oct4, Sox2, and Nanog. *Stem Cell Reports* **2:** 26–35.

Ralston A, Cox BJ, Nishioka N, Sasaki H, Chea E, Rugg-Gunn P, Guo G, Robson P, Draper JS, Rossant J. 2010. Gata3 regulates trophoblast development downstream of Tead4 and in parallel to Cdx2. *Development* **137:** 395–403.

Rayon T, Menchero S, Nieto A, Xenopoulos P, Crespo M, Cockburn K, Canon S, Sasaki H, Hadjantonakis AK, de la Pompa JL, et al. 2014. Notch and hippo converge on cdx2 to specify the trophectoderm lineage in the mouse blastocyst. *Dev Cell* **30:** 410–422.

Red-Horse K, Zhou Y, Genbacev O, Prakobphol A, Foulk R, McMaster M, Fisher SJ. 2004. Trophoblast differentiation during embryo implantation and formation of the maternal-fetal interface. *J Clin Invest* **114:** 744–754.

Reubinoff BE, Pera MF, Fong CY, Trounson A, Bongso A. 2000. Embryonic stem cell lines from human blastocysts: somatic differentiation in vitro. *Nat Biotechnol* **18:** 399–404.

Strumpf D, Mao CA, Yamanaka Y, Ralston A, Chawengsaksophak K, Beck F, Rossant J. 2005. Cdx2 is required for correct cell fate specification and differentiation of trophectoderm in the mouse blastocyst. *Development* **132:** 2093–2102.

Takahashi K, Yamanaka S. 2006. Induction of pluripotent stem cells from mouse embryonic and adult fibroblast cultures by defined factors. *Cell* **126:** 663–676.

Tanaka S, Kunath T, Hadjantonakis AK, Nagy A, Rossant J. 1998. Promotion of trophoblast stem cell proliferation by FGF4. *Science* **282:** 2072–2075.

Uy GD, Downs KM, Gardner RL. 2002. Inhibition of trophoblast stem cell potential in chorionic ectoderm coincides with occlusion of the ectoplacental cavity in the mouse. *Development* **129:** 3913–3924.

Wang J, Rao S, Chu J, Shen X, Levasseur DN, Theunissen TW, Orkin SH. 2006. A protein interaction network for pluripotency of embryonic stem cells. *Nature* **444:** 364–368.

Webb CF, Bryant J, Popowski M, Allred L, Kim D, Harriss J, Schmidt C, Miner CA, Rose K, Cheng HL, et al. 2011. The ARID family transcription factor bright is required for both hematopoietic stem cell and B lineage development. *Mol Cell Biol* **31:** 1041–1053.

Wheeler DL, Church DM, Federhen S, Lash AE, Madden TL, Pontius JU, Schuler GD, Schriml LM, Sequeira E, Tatusova TA, et al. 2003. Database resources of the National Center for Biotechnology. *Nucleic Acids Res* **31:** 28–33.

Whyte WA, Bilodeau S, Orlando DA, Hoke HA, Frampton GM, Foster CT, Cowley SM, Young RA. 2012. Enhancer decommissioning by LSD1 during embryonic stem cell differentiation. *Nature* **482:** 221–225.

Wu C, Orozco C, Boyer J, Leglise M, Goodale J, Batalov S, Hodge CL, Haase J, Janes J, Huss JW 3rd, et al. 2009. BioGPS: an extensible and customizable portal for querying and organizing gene annotation resources. *Genome Biol* **10:** R130.

Wu G, Gentile L, Fuchikami T, Sutter J, Psathaki K, Esteves TC, Arauzo-Bravo MJ, Ortmeier C, Verberk G, Abe K, et al. 2010. Initiation of trophectoderm lineage specification in mouse embryos is independent of Cdx2. *Development* **137:** 4159–4169.

Wu T, Wang H, He J, Kang L, Jiang Y, Liu J, Zhang Y, Kou Z, Liu L, Zhang X, et al. 2011. Reprogramming of trophoblast stem cells into pluripotent stem cells by Oct4. *Stem Cells* **29:** 755–763.

Zernicka-Goetz M, Morris SA, Bruce AW. 2009. Making a firm decision: multifaceted regulation of cell fate in the early mouse embryo. *Nat Rev Genet* **10:** 467–477.